Journal of Hydroscience and Hydraulic Engineering
Vol. 20, No.2 November, 2002, 71-82

BEHAVIOR OF FRESH AND SALT GROUNDWATER IN A SANDY COASTAL AQUIFER UNDER THE BEACH EROSION CONTROL USING PIPE DRAINS

By

Kei NAKAGAWA

Kyushu University, 6-10-1, Hakozaki, Higashi-ku, Fukuoka 812-8581, Japan

Tosao HOSOKAWA

Kyushu Sangyo University, 2-3-1, Matsukadai, Higashi-ku, Fukuoka 813-8503, Japan

Kousei IWAMITSU

Kyushu Sangyo University, 2-3-1, Matsukadai, Higashi-ku, Fukuoka 813-8503, Japan

Kenji JINNO

Kyushu University, 6-10-1, Hakozaki, Higashi-ku, Fukuoka 812-8581, Japan

and

Yoshinari HIROSHIRO

Kyushu University, 6-10-1, Hakozaki, Higashi-ku, Fukuoka 812-8581, Japan

SYNOPSIS

In order to protect sandy beaches from erosion caused by waves, a Beach Management System (BMS) is adopted in some areas along the Japanese coast. In order to predict the flow in the extended unsaturated zone due to increased drainage, numerical simulations were carried out for a laboratory aquifer and the cross section at a test site in Chiba Prefecture, Japan. The numerical simulations revealed that the unsaturated zone extends below the sandy beach, and that salt and fresh water mix around the drainpipes. In addition to the numerical simulations of fresh and saltwater movement, the water chemistry in the field aquifer is also presented by observation. The results of the chemical analysis indicated that the saltwater captured in the aquifer has considerably different properties than seawater due to the contact with the aquifer matrix for a long period and biochemical processes in the aquifer. An emphasis is put on the necessity of the combined study of physical and geochemical processes for a better understanding of the mechanism of saltwater intrusion.

INTRODUCTION

The Beach Management System (BMS) is a technique that utilizes drainpipes to increase seepage and sedimentation on the foreshore [1]. When the pipes constructed under a sandy beach are operated to drain groundwater, the unsaturated zone is extended and consequently a vertical flow toward the drainpipes is induced. The principle of BMS is to reduce the amount of water in the swash returning to the sea, resulting in an increase in the resisting force of the sand particles relative to the shear stress from the return flow. According to a review of Turner and Leatherman [2], the first study to propose that groundwater within beaches could be artificially manipulated to promote shoreline accretion was the laboratory study by Machemehl *et al.* [3]. Chappell *et al.* [4] were the first to experiment with pumping water out of natural beaches, and in 1983 the Danish Geotechnical Institute undertook the first prototype installation of a beach dewatering system at Hirtshals, Denmark. Bruun reported that the prototype installation could stabilize beach profile under mild wave condition, but that system could not stop beach erosion during storms [5]. Turner and Leatherman pointed out that an investigation into the dynamics of coastal groundwater determining the time-varying saturation characteristics of the beach face is important [1]. Further examination by field experiments and hydraulic model studies are necessary to do practical research on such beach stabilization.

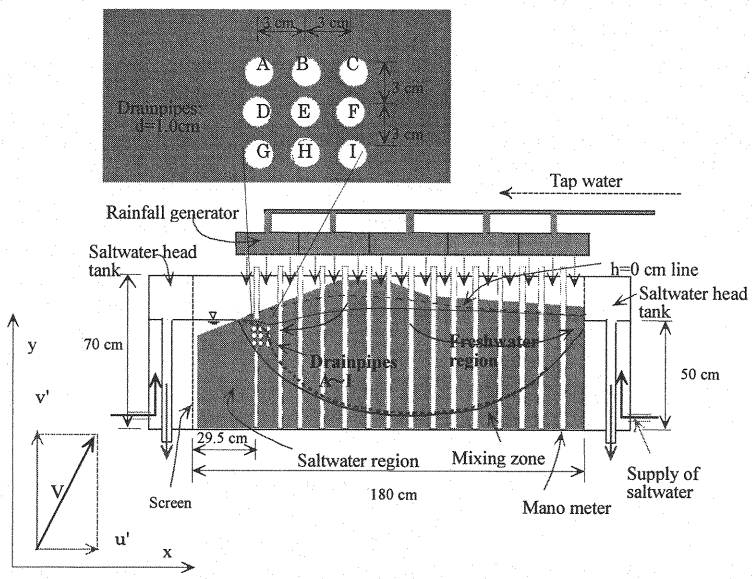

Figure 1 Experimental setup of laboratory aquifer

In order to design the appropriate depth, diameter, location, and discharge rate of the drainpipes, a numerical simulation to analyze the flow configuration in the unconfined aquifer would be highly useful. Sato *et al.* examined about beach transformation under coastal drain operation by experimental and numerical studies [6, 7]. They have shown an appropriate position of drainpipe and some characteristics of the system, with beach profile evolution. Chowdhury and Sato carried out two- and three- dimensional numerical analysis on the groundwater level that lowers by installing a permeable layer to the coastal aquifer [8]. However, their work did not include any details about the effects of mixing saltwater and fresh water. Water quality change such as salinity must be examined when collected water is utilized by facilities in the hinterland. Furthermore, the geochemical characteristics of the drained water to be released to the open water system should be carefully studied. In fact, the saltwater in the studied area located in Chiba Prefecture, Japan, is strongly reduced. This paper will deal with numerical simulations for laboratory and field experiments as well as the geochemical properties of the water.

LABORATORY EXPERIMENT OF SALTWATER INTRUSION WHEN GROUNDWATER IS DRAINED

In order to verify the accuracy of numerical model, the results of the model should be compared with results of laboratory experiment.

Fig.1 illustrates the cross section of the laboratory aquifer for which numerical simulations were carried out. The experimental setup is 2.0 m long, 0.7 m high and 0.125 m wide with the water tanks in both the right and left sides. Standard sand of 0.105-0.4 mm particle size was filled in the aquifer part of the setup, which is partitioned by tanks by wire gauze. The geometry of the sand aquifer with the slopes resembles a beach. At first, tap water was filled in the both side tanks and water depth sets to be 0.5 m. 10 mm h^{-1} constant tap water was infiltrated through the entire sand surface as rainfall, during whole day and night. Afterwards, tap water was replaced with saltwater in both side tanks. The salt water was colored with dye. Then, saltwater intrusion was observed. The density in the right and left boxes is maintained constant with the density equal to 1.025 kg l^{-1}. Saltwater progressed in wedge shape from both sides which coupled in 2880 minutes, forming what is known as a fresh water lens. Here, drainage by manifold drainpipes was carried out after the fresh water lens was formed. The change of the saltwater area was examined by a laboratory experiment and a numerical simulation. Installed 9 drainpipes were shown in Figure 1. The drainage experiment included 24 cases, which combined hydraulic head in pipes, position of operating pipes and the number of operating pipes. The behavior of the groundwater table and saltwater was photographed by a digital camera and an 8 mm video. Drainage discharge and density were then measured.

The following set of equations is applied for the numerical calculations:

Equation of unsaturated-saturated flow [9]

$$(C_w + \alpha_0 S)\frac{\partial h}{\partial t} = -\frac{\partial u}{\partial x} - \frac{\partial v}{\partial y} \quad , \quad u = -k\frac{\partial h}{\partial x} \quad , \quad v = -k\left(\frac{\partial h}{\partial y} + \frac{\rho}{\rho_f}\right) \tag{1}$$

Equation of mass conservation (Transport equation)

$$\frac{\partial(\theta c)}{\partial t} + \frac{\partial(u'\theta c)}{\partial x} + \frac{\partial(v'\theta c)}{\partial y} = \frac{\partial}{\partial x}\left(\theta D_{xx}\frac{\partial c}{\partial x} + \theta D_{xy}\frac{\partial c}{\partial y}\right) + \frac{\partial}{\partial y}\left(\theta D_{yy}\frac{\partial c}{\partial y} + \theta D_{yx}\frac{\partial c}{\partial x}\right) \tag{2}$$

where t is time, $h(x,y,t)$ is the piezometric head at the location of (x, y), k is the hydraulic conductivity, u and v are the velocity components in the x and y directions which are calculated by Darcy's law, ρ is the fluid density, ρ_f and ρ_s are the density of freshwater and saltwater, respectively, $C_w = d\theta/dh$ is the specific moisture capacity in unsaturated condition, S_s is the specific storage coefficient, α_0 is a dummy number which takes 0 in an unsaturated condition and 1 in a saturated condition, u' and v' are the components of real pore velocity in x and y directions calculated by $u' = u/\theta$ and $v' = v/\theta$.

The dispersion coefficients, which are dependent on the real pore velocity, are represented as follows [10] :

$$\theta D_{xx} = \frac{\alpha_L u'^2}{V} + \frac{\alpha_T v'^2}{V} + \theta D_M \ , \ \theta D_{yy} = \frac{\alpha_T u'^2}{V} + \frac{\alpha_L v'^2}{V} + \theta D_M \ , \quad \theta D_{xy} = \theta D_{yx} = \frac{(\alpha_L - \alpha_T)u'v'}{V} \tag{3}$$

where α_L and α_T are the microscopic dispersivity for longitudinal and transverse directions related to the sand particle diameter, $V = \sqrt{u'^2 + v'^2}$, and D_M is the fluid molecular diffusion coefficient.

The saltwater concentration c (x,y,t) in (2) is related to the change in the saltwater density through:

$$c(x,y,t) = \frac{100[\rho(x,y,t) - \rho_f]}{(\rho_s - \rho_f)} \tag{4}$$

It is necessary to show the relationship between the negative pressure head h and the volumetric water content θ, ratio of saturated hydraulic conductivity k_s and unsaturated hydraulic conductivity k and specific moisture capacity C_w are as unsaturated characteristics of the aquifer, in order to carry out the numerical simulation including the unsaturated zone. In this paper, unsaturated values were obtained from the theoretical formula of van Genuchten (5) [11].

$$S_0 = \frac{\theta - \theta_r}{\theta_s - \theta_r} \quad , \quad S_e = \left[\frac{1}{1 + (\alpha|h|)^n}\right]^m$$
$$k_r = S_0^{1/2}\left\{1 - \left(1 - S_e^{1/m}\right)^m\right\}^2 \tag{5}$$
$$C_w = \frac{\alpha \cdot m(\theta_s - \theta) S_e^{1/m}\left(1 - S_e^{1/m}\right)^m}{1 - m}$$

where θ_r is the residual water content, θ_s is the saturated water content and α, m and n are the coefficients of the van Genuchten formula. In the numerical simulation, successive over relaxation (SOR) method was used to solve equation (1) and the method of characteristics (MOC) was used to solve equation (2) [12].

Lower end boundary conditions for groundwater flow and transport calculations were set to be impermeable and no gradient of concentration, respectively. Fresh water recharge from sand surface was 8 mm h^{-1}. Boundary conditions of concentration for seaside (left side), sea bed and river side (right side) were as follows: When the flow of boundary toward to inside of numerical area, concentration should be 100 %. When the flow of boundary toward to outside of numerical area, concentration should have no gradient. Hydraulic conditions of these boundaries were hydrostatic pressure conditions. At the bottom of numerical

area, impermeable and 0 % concentration boundary conditions were given. At the soil surface, 8 mm h^{-1} recharge quantity and 0 % concentration boundary condition were given.

Table 1 Simulation conditions for laboratory experiment

Hydraulic Conductivity k (cm s^{-1})	5.0×10^{-2} (upper) 3.7×10^{-2} (lower)
Longitudinal dispersivity α_L (cm)	0.034
Transversal dispersivity α_T (cm)	0.0034
Grid size in x direction Δx (cm)	1.0
Grid size in y direction Δy (cm)	0.5
Unsaturated flow property for van Genuchten model	
θ_s	0.450
θ_r	0.108
α (cm^{-1})	0.051
n	10.53

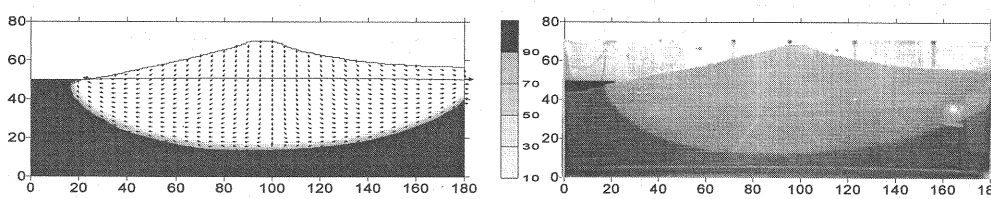

Figure 2 Initial condition of drainage (left: numerical, right: experimental)

The conditions of laboratory experiment were used as numerical conditions as listed in Table 1. The values of the standard sand were used for saturated hydraulic conductivity and unsaturated parameters. Numerical simulation on the drainage was carried out for 24 cases as well as a laboratory experiment. The results of our experiment and numerical simulation also agreed well on all cases. The numerical results of main cases are summarized as follows:

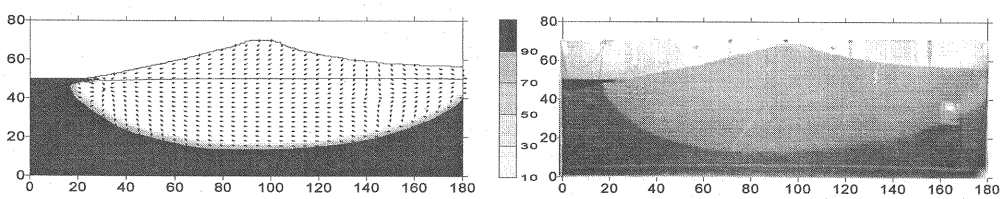

(a) 10 min

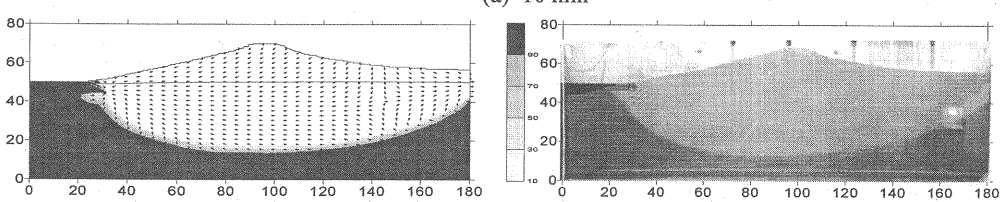

(b) 46 min

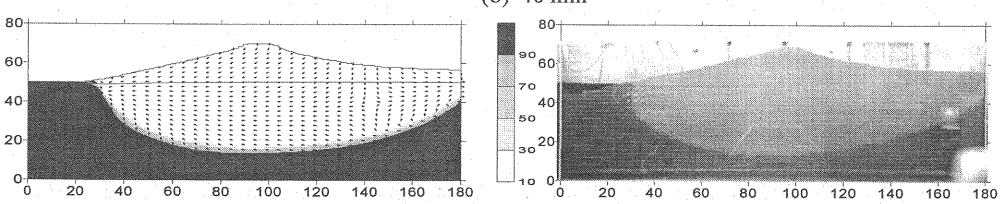

(c) 120 min

Figure 3 Numerical results (left) of B-drainage case compared with experimental results (right)

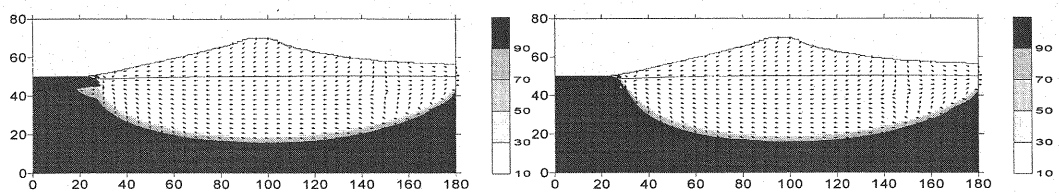

Figure 4 Numerical results of AB-drainage case (left: 26 min, right: 82 min)

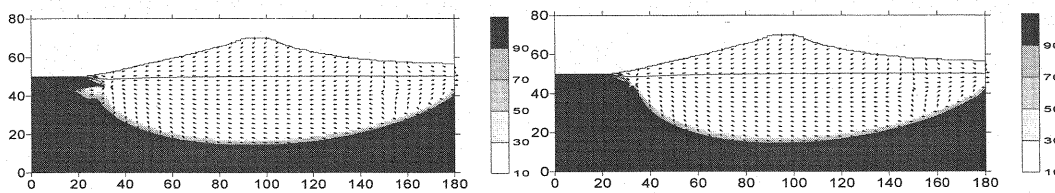

Figure 5 Numerical results of BC-drainage case (left: 40 min, right: 120 min)

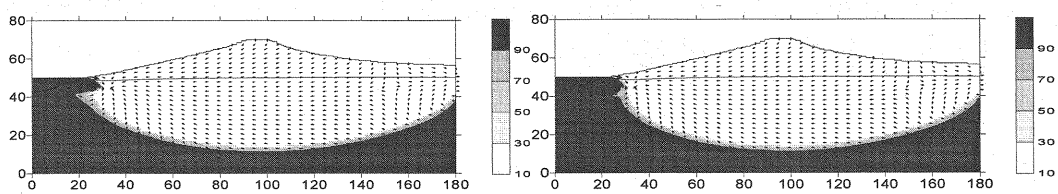

Figure 6 Numerical results of ABC-drainage case (left: 20 min, right: 44 min)

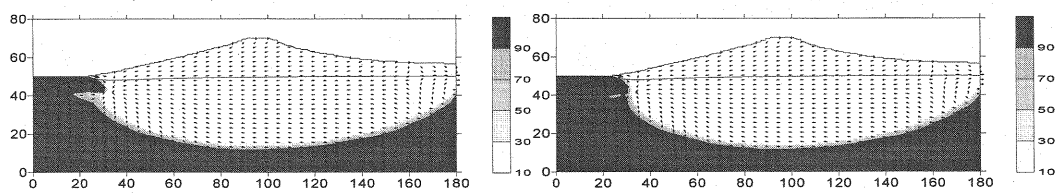

Figure 7 Numerical results of DEF-drainage case (left: 14 min, right: 28 min)

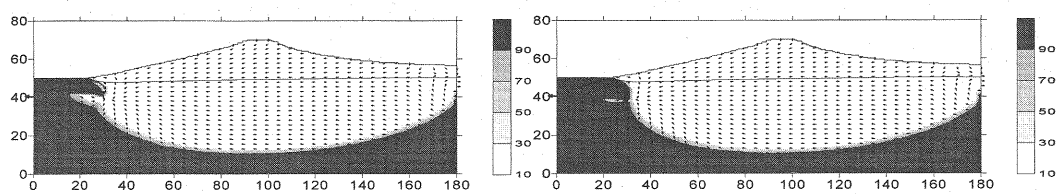

Figure 8 Numerical results of GHI-drainage case (left: 10 min, right: 24 min)

Initial condition for all cases is shown in Fig.2. In case of drainage from B (hydraulic head: 48.0 cm, Fig. 3), saltwater area extends to the upper part of the drainpipes from the left side saltwater tank. After that, the saltwater area of the lower part extended toward drainpipes. The direction of saltwater from the lower part of drainpipes was reversed after intruded horizontally. Saltwater came from upper half of the left side boundary flown toward drainpipes directly. Saltwater from the right side boundary intruded into the central part of the aquifer horizontally and afterwards, the direction gradually changed and moved upward toward the drainpipes. The fresh water from left side of 3/4 in sand surface headed for the drainpipes. On the other hand, fresh water from right side of 1/4 in sand surface joined fresh water in the aquifer, and was flown out to the right side boundary along the groundwater table. Numerical results agreed well with experimental results.

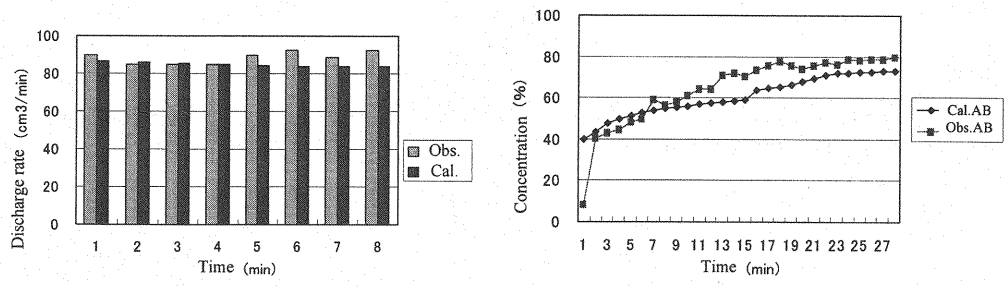

Figure 9 Drainage discharge and concentration of ABC-drainage case
(left: discharge, right: concentration of AB)

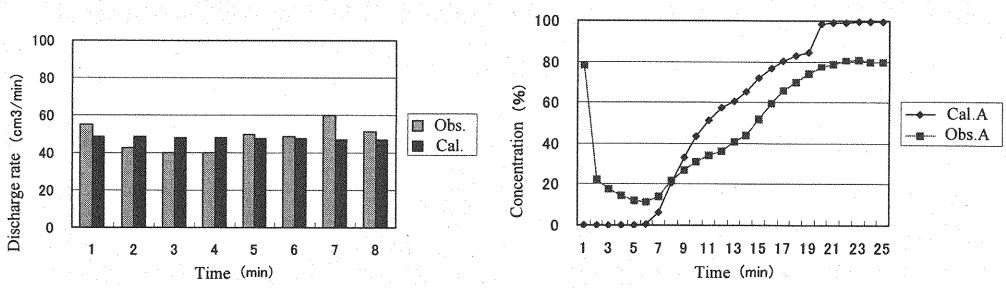

Figure 10 Drainage discharge and concentration of AB-drainage case
(left: discharge, right: concentration of A)

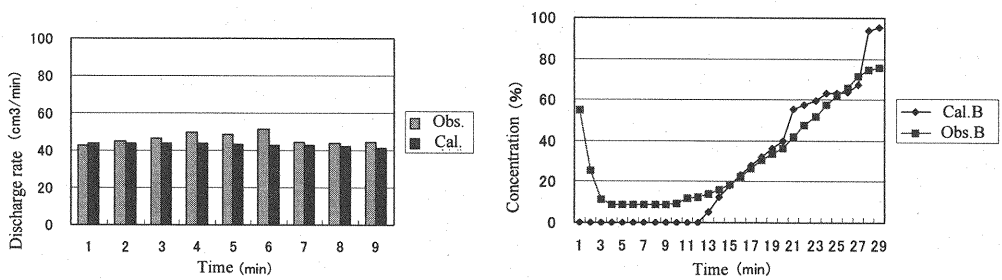

Figure 11 Drainage discharge and concentration of BC-drainage case
(left: discharge, right: concentration of B)

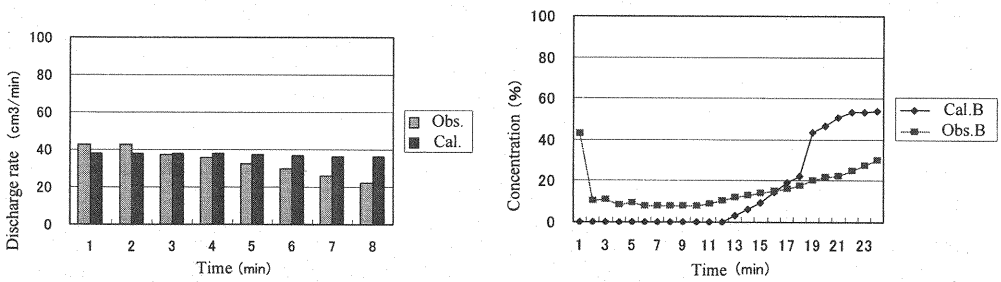

Figure 12 Drainage discharge and concentration of B-drainage case
(left: discharge, right: concentration)

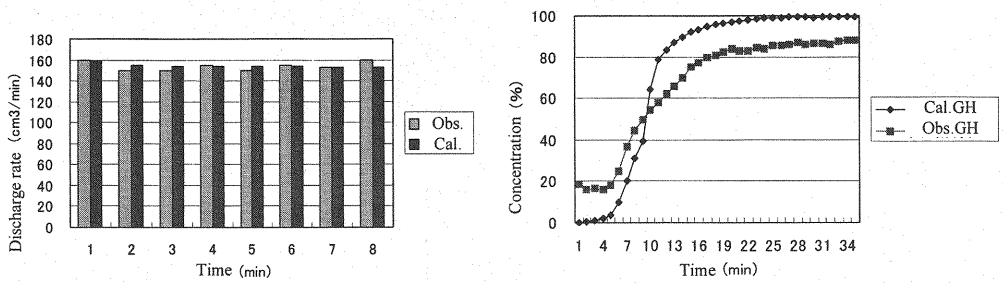

Figure 13 Drainage discharge and concentration of GHI-drainage case
(left: drainage, right: concentration of GH)

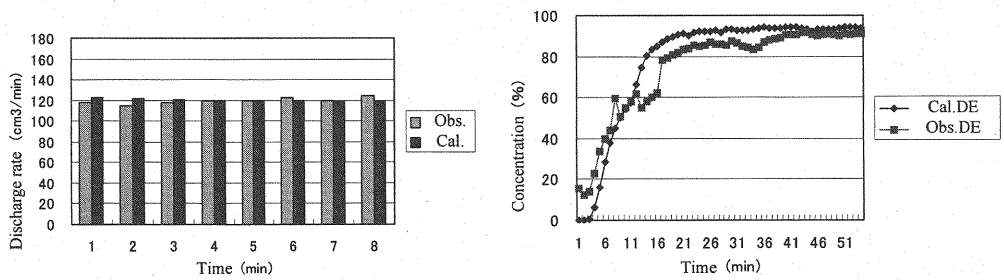

Figure 14 Drainage discharge and concentration of DEF-drainage case
(left: discharge, right: concentration of DE)

In case of drainage from AB (hydraulic head: 48.0 cm, Fig. 4), the extension speed of saltwater area was larger than B-drainage case, because the hydraulic gradient of this case was larger than B-case due to the fact that drainpipes were close to the left side boundary.

In case of drainage from BC (hydraulic head: 48.0 cm, Fig. 5), the extension speed of saltwater area was smaller than AB-drainage case, because hydraulic gradient of this case was smaller than AB-case due to the fact that the drainpipes were far from left side boundary.

In case of drainage from ABC (hydraulic head: 48.0 cm, Fig. 6), the extension speed of the saltwater area was faster than the above cases, because the drainage discharge was larger than the above cases.

In case of drainage from DEF (hydraulic head: 47.0 cm, Fig. 7), the extension speed of saltwater area was larger than ABC-drainage case because hydraulic head was lower than the ABC-case.

In case of drainage from GHI (hydraulic head: 46.0 cm, Fig. 8), the extension width and speed of saltwater area was largest of all cases, because hydraulic head was lowest and the position of drainpipes is the highest of the all cases.

In the above cases, fresh/saltwater flow pattern and extent shape of saltwater area in the final stage were all similar to B-drainage case.

Next, changes of drainage discharge and concentration were as follows: When the drainpipes elevation and hydraulic head were the same, drainage discharge of ABC (Fig. 9), AB (Fig. 10), BC (Fig. 11), and B (Fig. 12) was abounding in order, and concentration also rose rapidly in the same order. The drainage concentration of cases of 2 or 3 pipes was higher than the case of just one pipe case. When the number of drainpipes was the same, drainage discharge of GHI (Fig. 13), DEF (Fig. 14) and ABC was abounding in order. The maximum drainage concentration was high at almost the same order of that. The drainage discharge and concentration of numerical results of above cases were good agreement with experimental one.

The following conclusions can be drawn from this study:

1. Accurate numerical results of the laboratory experiments were obtained.
2. The unsaturated zone increases when a BMS is operated.
3. The drained water is mixed with saltwater.
4. The concentration of drained water depends on the configuration of the pipes.

The present numerical simulation is applicable to the design of a BMS, if sufficient information on the parameter values necessary for the modeling is available *a priori*.

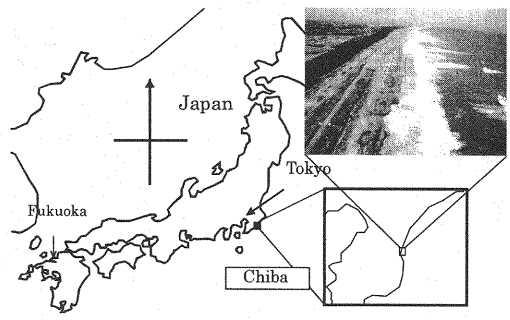

Figure 15 BMS test site in Chiba, Japan

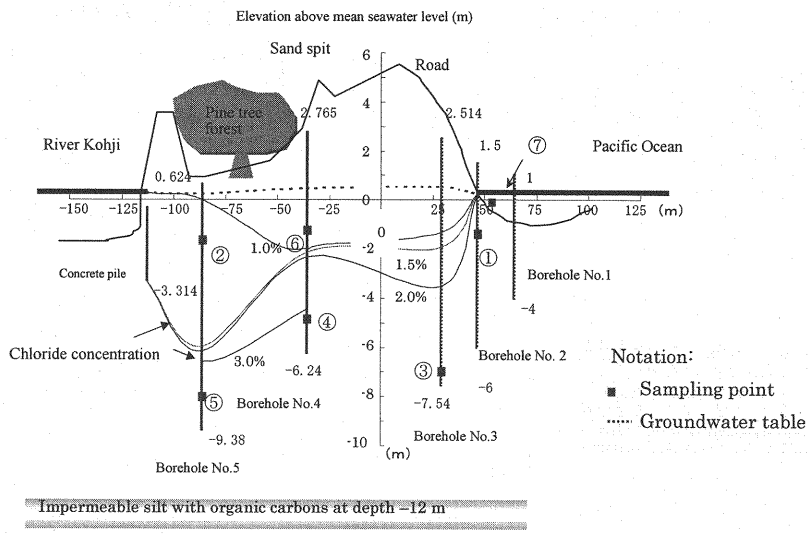

Figure 16 Beach cross section at the test site

TOPOGRAPHIC AND GEOLOGICAL CONDITIONS AT THE TEST SITE

After the accuracy of the present model was verified for the transient behavior of fresh and saltwater in the laboratory experiment, a simulation for full-scale conditions was carried out. However, the effect of waves upon the infiltration to the drainpipes, especially the waves in the swash zone, was not incorporated in the present simulation.

Fig.15 is the test site at Ichinomiya Beach in Chiba Prefecture, Japan. The sand beach extends as shown in the picture of the site. Fig. 16 depicts the typical cross section of the beach where the BMS test is being carried out. Vertical lines show boreholes from no. 1 to no. 5 and sampling points show from ① to ⑥. The sand spit was formed on an alluvial deposit contaminated with much dissolved organic carbon. This deposit primarily functions as an impervious layer. The unconfined groundwater table, electric conductivity (chloride concentration), the tidal variation, and other meteorological factors were observed. Fig.17 displays a part of such observation series. The positions of drainpipes are as shown in Fig. 18. It can be seen that the groundwater table at No.3 and 5 are remarkably affected by the tidal fluctuation, while No. 4 does not show so many effects. The groundwater table rises when it rains. It is thought that the declivous tendency of groundwater table is due to the BMS operation. Moreover, as a result of a field survey, it was observed that the water in the swash on the site of the BMS infiltrated quickly.

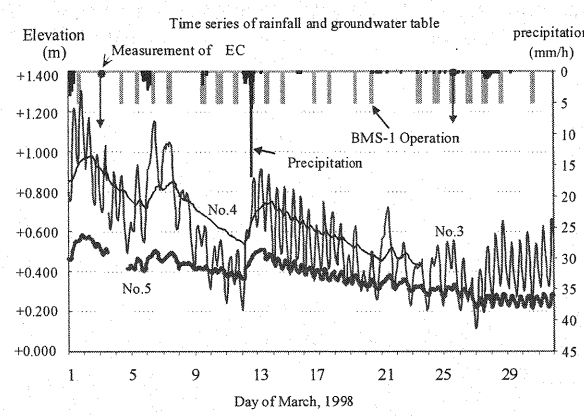

Figure 17 Time series of precipitation and groundwater levels

Table 2 Simulation conditions for test site

Hydraulic Conductivity k (cm s^{-1})	3.7×10^{-2}
Longitudinal dispersivity α_L (cm)	0.36
Transversal dispersivity α_T (cm)	0.036
Grid size in x direction Δx (cm)	100
Grid size in y direction Δy (cm)	20
Unsaturated flow property for van Genuchten model	
θ_s	0.342
θ_r	0.075
α (cm^{-1})	0.0491
n	7.137

RESULT OF NUMERICAL SIMULATIONS

Table 2 shows the numerical simulation conditions. The saturated hydraulic conductivities were obtained from laboratory hydraulic conductivity tests using sand of the test site. Since unsaturated parameters used in equation (5) have not been obtained, the parameters of the general sandy soil were used. A constant precipitation rate of 2 mm day^{-1} was assumed, and the tide was set equal to the mean seawater level. The water head in the drainpipes, when BMS was operated, was adjusted so that the total discharge from the four drainpipes calculated by the model met the observed discharge. Fig.18 depicts the flow pattern and the concentration distribution for steady-state conditions. Saltwater detoured under the sheet pile, because the river side (left side) boundary was also made to be saltwater boundary. Saltwater intrusion occurred and fresh water lens formed. In unsaturated zone, fresh water flows vertically from sand surface to groundwater table. The present model may be used to describe the fundamental characteristics of the flow by making a comparison between Figs. 16 and 18. Fig.19 shows the calculated chloride profile at the boreholes. Except for the fluctuation of the vertical displacement in the mixing zone, the simulated result almost coincides with the observations. The observed chloride concentration at the groundwater table of No.3 and No.5 is higher compared to the observed and calculated values at No.4. The reason for this is that the concentration in boreholes No.3 and No.5 is affected by seawater spray, which may infiltrate like rainwater when it is windy and wavy. A reasonable agreement is found at No.4 since the hole is not affected to the same degree by spray. Fig. 20 yields a close view of the flow 24 hours after the BMS operation started. The flow pattern in the mixing zone has changed. The chloride contaminated the drained water, and it was observed that the groundwater table was lower as 50 cm within 15 m from the coastal line and that unsaturated region expanded, in 24 hours.

GEOCHEMICAL PROPERTIES OF SALTWATER IN THE AQUIFER

Geochemical analyses were conducted, because the drained water can be used for other purposes such as in swimming pools and as a heat source. As shown in Table 3, a significantly reduced environment is

anticipated due to low dissolved oxygen, low oxidation-reduction potential, and low sulfate. It is therefore necessary to account for the hydro-geochemical processes in the simulation model [13]. However, this is a subject for future studies.

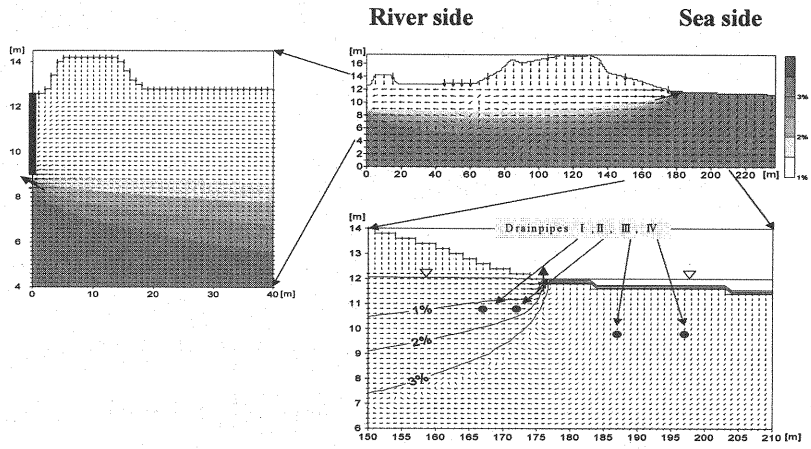

Figure 18 Steady state of fresh and saltwater flow before BMS is operated

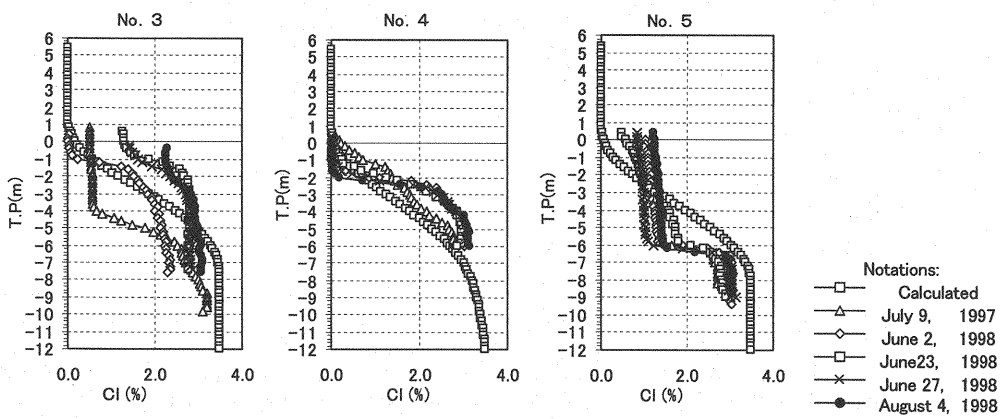

Figure 19 Calculated and observed chloride concentrations

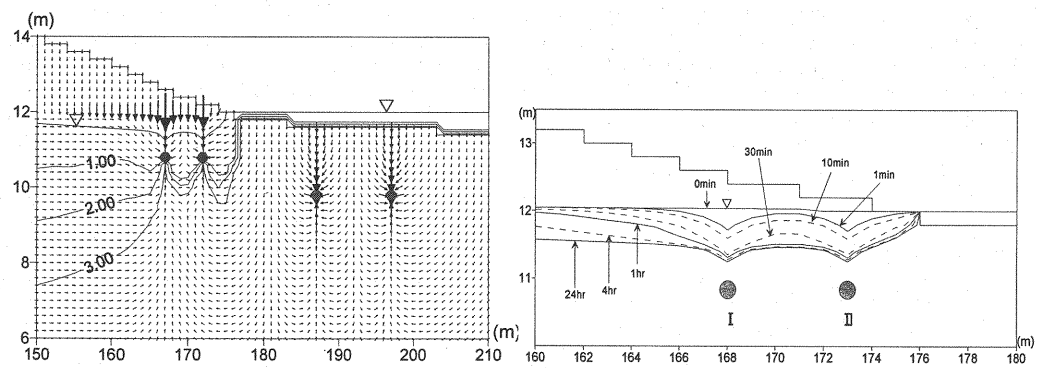

Figure 20 Change in the chloride profile and unsaturated zone when BMS is operated
(left: 24hors after operation started, right: water table near the drainpipes)

Table 3 Some chemical components of fresh and saltwater in the aquifer

Date of sampling	12 Aug 97		2 Jun 98			2 Aug 98	
Sampling Point	No. 2 B.H. (salt water)	No. 5 B.H. (fresh water)	No. 3 B.H. (salt water)	No. 4 B.H. (salt water)	No. 5 B.H. (salt water)	No. 4 B.H. (fresh water)	Salt water
Point	TP -1.380	TP -1.620	TP -6.941	TP -5.835	TP -7.976	TP -1.235	TP +0.000
	①	②	③	④	⑤	⑥	⑦
pH(℃)	8.1(24)	7.9(24)	8.2(18)	7.2(18)	6.9(18)	7.6(23)	7.7(23)
Na^+(mg/l)			4500	5900	5500	120	10000
K^+ (mg/l)			170	220	210	15	380
Ca^{2+} (mg/l)			190	240	220	45	380
Mg^{2+} (mg/l)			480	650	620	39	1100
Fe^{2+} (mg/l)			<0.1	0.2	<0.1	<0.1	<0.1
Total-Mn (mg/l)			0.06	1	0.17	0.04	<0.01
Cl^- (mg/l)			7300	9500	9100	230	16000
SO_4^{2-} (mg/l)			1000	1200	980	40	2300
DO (mg/l)	1.7	<0.5	(4.1)	(2.9)	<0.5	3.5	7.4
DOC (mg/l)			5	5	11	<1	2
TOC (mg/l)			7	14	20	1	2
Eh (mV)			-66	-99	-380	78	18
PO_4-P (mg/l)	0.045	0.25	0.17	0.13	0.39	0.038	0.023
Total-P (mg/l)	0.078	0.33	0.24	0.24	0.74	0.11	0.057
S^{2-} (mg/l)			<0.5	<0.5	11	<0.5	<0.5
COD (mg/l)	3.1	7.6					
NO_2-N (mg/l)	0.26	0.011					
NO_3-N (mg/l)	0.35	0.03					
Odor	No odor	Slight odor of H_2S					

CONCLUSIONS

Based on the laboratory experiment, findings demonstrated that the model proposed in this study is suitable for the primary analyses of the flow and concentration distribution when the BMS is operated. Field tests revealed similar behavior as observed in the laboratory experiment. However, the boundary and hydrological conditions need to be improved in order to simulate more practical situations. Furthermore, it should be emphasized that geochemical considerations are indispensable for a better understanding of saltwater intrusion in aquifers.

ACKOWLEDGEMENTS

The authors express the deepest gratitude to the Japanese Public Works Research Center for granting permission to use the field data. The authors would also like to thank Dr. Magnus Larson of Lund University, Sweden, who provided valuable comments on this paper. The authors also wish to thank Mr. Masahiko Ohgushi and Mr. Jynpei Nishihara for their assistance in laboratory experiments and numerical simulations.

REFERENCES

1. Charlier, R.H. and C.P. De Meyer: Ask Nature to Protect and Build-up Beaches, *Journal of Coastal Research*, Vol.16, No.2, pp.385-390, 2000.
2. Turner, I.L. and S.P. Leatherman: Beach Dewatering as a 'Soft' Engineering Solution to Coastal Erosion-A History and Critical Review, *Journal of Coastal Research*, Vol.13, No.4, pp.1050-1063, 1997.
3. Machemehl, J.L., T.J. French and N.E. Huang: New method for beach erosion control, *Proceedings: Engineering in the Oceans, American Society of Civil Engineers Specialty Conference*, pp.142-160, 1975.
4. Chappell, J., I.G. Eliot, M.P. Bradshaw and E. Lonsdale: Experimental control of beach face dynamics by watertable pumping, *Engineering Geology*, Vol.14, pp.29-41, 1979.
5. Bruun, P.: The Coastal Drain: What Can It Do or Not Do?, *Journal of Coastal Research*, Vol.5, No.1, pp.123-125, 1989.
6. Sato, M., S. Hata and M. Fukushima: An experimental study on beach transformation due to waves under the operation of coastal drain system, *Proc. 24th ICCE.*, pp.2571-2582, 1994.
7. Sato, M., T. Fukushima, R. Nishi and M. Fukunaga: On the change of velocity field in nearshore zone due to coastal drain and the consequent beach transformation, *Proc. 26th ICCE.*, pp.2666-2676, 1996.
8. Chowdhury, S.A. and M. Sato: On preferable location of a dewatering system in a sandy beach, *Coastal Engineering V Computer Modelling of Seas and Coastal Regions*, pp.23-30, 2001.
9. Hosokawa, T., K. Jinno and K. Momii: Estimation of transverse dispersivity in the mixing zone of fresh-salt groundwater, *Calibration and reliability in Groundwater Modeling*, IAHS Publ. No.195,

pp.149-158, 1990.
10. Huyakorn, P.S. and G.F. Pinder: *Computational method in subsurface flow*, Academic Press, NewYork, 1983.
11. van Genuchten: A closed-form equation for predicting the hydraulic conductivity of unsaturated soils, *Soil Science Society of America Journal*, Vol. 44, pp.893-898, 1980.
12. Pinder, G.F. and H.H. Cooper: A numerical technique for calculating the transient position of the saltwater front, *Water Resources Research*, Vol.6, No.3, pp.875-882, 1970.
13. Hiroshiro, Y., K. Jinno, S.-I. Wada, T. Yokoyama, and M. Kubota: Multicomponent solute transport model with cation exchange in a redox subsurface environment, *Calibration and reliability in Groundwater Modeling*, IAHS Publ. No. 265, pp.474-480, 2000.

APPENDIX-NOTATION

The following symbols are used in this paper:

c	=	saltwater concentration;
C_W	=	specific moisture capacity;
D_M	=	fluid molecular diffusion coefficient;
h	=	piezometric head;
k	=	hydraulic conductivity;
k_s	=	saturated hydraulic conductivity;
S_S	=	specific storage coefficient;
t	=	time;
u,v	=	Darcy's velocity for x and y directions;
u', v'	=	real pore velocity for x and y directions;
V	=	real pore velocity for fluid flow direction;
α, m and n	=	coefficients of van Genuchten formula;
α_0	=	dummy number that takes 0 in unsaturated condition and 1 in saturated condition;
α_L, α_T	=	microscopic dispersivity for longitudinal and transverse directions;
θ_r	=	residual water content;
θ_s	=	saturated water content; *and*
ρ, ρ_f and ρ_s	=	density of fluid, density of fresh water and density of saltwater.

(Received June 5, 2002 ; revised September 10, 2002)